Nature Environment and Pollution Technology
An International Quarterly Scientific Journal

p-ISSN: 0972-6268
(Print copies up to 2016)
e-ISSN: 2395-3454

Vol. 24 | No. 4 | Article ID B4298 | 2025

Original Research Paper

https://doi.org/10.46488/NEPT.2025.v24i04.B4298

Open Access Journal

A Comparative Study of Statistical and Machine Learning Modelling Techniques in Air Pollution Data

Sumithra Palraj[1]†, Loganathan Appaia[2], Deneshkumar Venugopal[3] and Gunasekaran Munian[4]

[1]Department of Statistics, Pondicherry University, Pondicherry-605 001, India
[2]Department of Statistics, Central University of Tamil Nadu, Thiruvarur-610005, Tamil Nadu, India
[3]Department of Statistics, Manonmaniam Sundaranar University, Tirunelveli-627012, Tamil Nadu, India
[4]Department of Applied Research, The Gandhigram Rural Institute (Deemed to be University), Dindigul-624 302, Tamil Nadu, India
†Corresponding author: Sumithra Palraj; 350433@msuniv.ac.in

Abbreviation: Nat. Env. & Poll. Technol.
Website: www.neptjournal.com

Received: 18-12-2024
Revised: 07-02-2025
Accepted: 16-02-2025

Key Words:

Autoregressive moving average
Facebook Prophet method
Long short-term memory
Air Quality Index

Citation for the Paper:

Palraj, S., Appaia, L., Venugopal, D. and Munian, G. 2025. A comparative study of statistical and machine learning modelling techniques in air pollution data. *Nature Environment and Pollution Technology*, 24(4), B4298. https://doi.org/10.46488/NEPT.2025.v24i04.B4298

Note: From 2025, the journal has adopted the use of Article IDs in citations instead of traditional consecutive page numbers. Each article is now given individual page ranges starting from page 1.

ABSTRACT

Different approaches are being adopted in practice for determining models for given time series. The approaches can be categorized broadly into three, viz., statistical, machine learning and deep learning. Since they differ with respect to their theoretical base, their outcomes also differ. Decision-making based on the values predicted from the time series models seeks the accuracy of the forecast values. This paper studies the effectiveness of the three approaches by comparing the performance of the autoregressive moving average method developed by applying statistical principles, the Facebook Prophet method developed from a Machine Learning approach and the long short-term memory method developed from deep learning. The study is carried out for real data of time series of air quality indices.

INTRODUCTION

One of the main applications of time series models is forecasting values with a desired level of accuracy based on the observations available for the past time periods. This is crucial for decision-making in various fields, as it allows for the prediction of future trends and patterns and the identification of potential risks and opportunities. Buyuksahin & Ertekin (2019) have mentioned that time series models can also be used to extract meaningful information from a large amount of data and to identify underlying relationships and patterns in the data. In recent years, there has been a significant amount of research on developing methods for time series modelling, applying machine learning and deep learning approaches. These methods can handle large, complex datasets. Parmezan et al. (2019) have pointed out that the models developed from these approaches can identify patterns and trends, which may be difficult to discern using conventional statistical methods.

It is well known that the autoregressive moving average/autoregressive integrated moving average (ARIMA/ARMA) methods have been developed based on statistical principles (Box et al. 1970), and the outcomes of the models possess desirable theoretical properties. Machine learning techniques, such as support vector machine (SVM) and random forests, have also been shown to be effective in forecasting time series data. Deep learning methods, such as the long short-term memory (LSTM) method, have demonstrated the ability to handle large amounts of data and capture complex relationships in the data (Toharudin et al. 2020).

Current research in time series modeling has also focused on improving the accuracy and efficiency of forecasting methods. Calvo & Santafé Rodrigo (2016)

have mentioned that different time series modelling methods can be compared to various features such as seasonality, trend, level, noise, etc., of the time series data, ability to handle different types of data, computational complexity of the methods, as well as the interpretability of the results and accuracy of the forecast values.

In recent years, air pollution has become a major concern for cities and communities around the world. Increasing levels of toxic substances in the air have caused a wide range of health problems, from respiratory issues to heart disease. The most common sources for air pollution include industrial emissions, transportation and energy production. As a result, the public is breathing polluted air every day, leading to a rise in respiratory diseases and other illnesses. Though industrial growth leads to economic development of a nation, it also returns poor quality air to humankind. Hence, there is a considerable amount of consideration worldwide for discussing Climate Change. Analysis of information about the contents of air, which all human beings inhale, is pertinent in view of the health of the public. In recent years, several studies have examined the use of ARIMA models for forecasting air pollutant concentrations.

Samia et al. (2012) conducted a study to predict the levels of PM10 over a 24-hour period in Tunisia. They proposed a hybrid method, which combines the ARIMAX and artificial neural network (ANN) models with a multilayer perceptron architecture. This model was able to identify both linear and non-linear time series patterns effectively, making it a valuable tool for forecasting and early warning systems. Haviluddin et al. (2015) compared the performance of the ARIMA method, Back-Propagation Neural Network (BPNN) and genetic algorithms for analyzing and predicting short-term time series network traffic activity datasets. They experienced that BPNN is efficient in learning time series data. Naveen & Anu (2017) compared the effectiveness of ARIMA and Seasonal ARIMA models for forecasting ambient air quality data in Thiruvananthapuram District, Kerala, India, and found that the ARIMA model performed better. Patra (2017) used a combination of the ARIMA method and artificial intelligence techniques like ANN and SVM to predict the concentration of atmospheric pollutants in India and obtained satisfactory results with the ARIMA model.

Abhilash et al. (2018) found that the ARIMA model is effective for short-term forecasting of nitrogen dioxide (NO_2), PM_{10} and sulfur dioxide (SO_2) for the data of Bengaluru city.

Parmezan et al. (2019) compared the effectiveness of the four algorithms, viz., ANN, SVM, kNN-TSPI and SARIMA, in predicting trends in multi-step-ahead projections with approximate or updated iterations. Their results showed that the kNN-TSPI method has notable stability and robustness in forecasting as accurately as SARIMA and SVM, but with the added advantage of being easier to understand, implement, and modify with only two input parameters that can be easily determined based on seasonal patterns in the data. These findings suggest that machine learning methods have reached a similar level of maturity to statistical models in temporal data modelling.

In a study by Samal et al. (2019), the SARIMA and Prophet models were evaluated for predicting pollution in Bhubaneswar City using historical data. These methods were found, based on various performance measures, to achieve high levels of accuracy. Particularly, the Prophet model with log transformation was found to be relatively more effective for forecasting future pollution levels in Bhubaneswar City.

In the study by Toharudin et al. (2020), the LSTM and the Prophet models were used to analyze historical data of daily maximum and minimum air temperatures in Bandung. Their findings showed that the Prophet model performs relatively better for forecasting maximum air temperature, while the LSTM model performs relatively better for forecasting minimum air temperature. Sanchez-Pozo et al. (2021) compared the accuracy in the forecast values of Ozone (O_3) concentration for assessing the air quality of London city, obtained from the four forecasting models: Facebook Prophet (Prophet), LSTM, Support Vector Regression (SVR) and ARIMA. They observed that the LSTM model achieved the highest accuracy among the models considered. Some works could be found in the literature on studying the quality of air and chemical pollutants causing air pollution in Chennai, a metropolitan city in India. Nadeem et al. (2020), applying the ARIMA method, developed nine univariate linear stochastic models for forecasting the concentration levels of the chemical pollutants, viz., respirable suspended particulate matter, SO_2 and NO_2 in three areas of Chennai city. Ammasi Krishnan et al. (2020) found that the level of $PM_{2.5}$ is three times higher than the National Ambient Air Quality Standard (NAAQS) of India, while other pollutants are within acceptable limits, during Diwali days.

Angelena et al. (2021) examined the concentration of PM10 in the four locations, Anna Nagar, Adyar, Thiyagaraya Nagar & Kilpauk of Chennai city, applying a neural network with a multilayer feed-forward backpropagation method. Whereas Janarthanan et al. (2021) found that a combination of the deep learning model based on LSTM and SVR could accurately predict the air quality index (AQI) of some locations of Chennai. Mani & Volety (2021), applying the LSTM and ARIMA methods, predicted the levels of air pollutants and found that the LSTM model

produced relatively precise results than the ARIMA model.

Varma et al. (2021) investigated and analyzed the concentration of suspended PM and its associated health consequences in five locations: Alandur, Marina Beach Road, Velachery, Koyambedu and Anna Salai of Chennai city. They discovered that out of the five locations, Alandur, Marina Beach Road and Velachery have moderate AQI values, while Koyambedu and Anna Salai have poor AQI values. Recently, Gunasekar et al. (2022) proposed a novel and optimized deep learning algorithm, which combines ARIMA and CNN-LSTM methods for forecasting the AQI of Chennai with a higher level of accuracy.

It can be noted, in general, from the above discussions that the performance of the approaches or methods applied for time series modelling is data-dependent. AQI time series is challenging to handle due to its inherent complexity, nonstationary, and susceptibility to external factors such as weather conditions, seasonal variations and human activities. These factors cause patterns to shift unpredictably, making it difficult to model and forecast accurately. Unlike other types of data, air pollution data often exhibits irregular trends, sudden spikes, and long-term dependencies, which require specialized techniques to capture and analyze effectively. Addressing these patterns is crucial because accurate forecasting of air pollution levels enables proactive measures to mitigate health risks, inform public policy, and improve environmental management.

Hence, it has become essential to identify an appropriate approach or method for designing effective forecasting models for every location. The main objective of this work is to identify an effective method for forecasting the AQI of Chennai city by comparing the performance of three methods, viz., ARIMA, Prophet, and LSTM, evolved respectively from statistical, machine learning and deep learning approaches. Implements these three distinct methodologies for time series analysis: ARIMA, LSTM and Prophet. Each methodology was selected based on unique capabilities in addressing specific aspects of time series analysis and forecasting challenges.

The ARIMA methodology demonstrates proven effectiveness in modeling linear relationships and handling datasets with distinct trends and seasonality patterns. This approach combines autoregressive and moving average components, utilizing differencing techniques to achieve data stationarity. Through systematic parameter tuning and iterative testing processes, the model specifications were established for accurate forecasting capabilities.

For addressing non-linear and complex patterns, the LSTM architecture leverages advanced capabilities in modeling long-term dependencies within sequential data. The network architecture incorporates multiple layers with carefully configured neurons across input, hidden and output layers. The implementation includes optimized hyperparameters and activation functions, ensuring effective information flow and gradient management throughout the training process while maintaining computational efficiency and preventing model overfitting.

Facebook Prophet methodology addresses multiple seasonal patterns and irregular events within the time series data. This sophisticated approach incorporates automated detection mechanisms for various seasonality patterns while effectively managing holiday effects and outlier scenarios. The model's configuration includes robust outlier handling mechanisms and flexible seasonality modeling, providing significant advantages over traditional forecasting approaches.

During the COVID-19 Lockdown, the air pollution levels were significantly lower. The primary reason for this reduction was the drastic decrease in vehicular movement due to strict lockdown measures. With fewer vehicles on the road, industrial activity also slowed down, leading to minimal fluctuations in air pollution data.

Since time series models rely on variations in data to make accurate predictions, the lockdown period, characterized by consistently low pollution levels, does not provide meaningful insights for model comparison. Instead, we focused on the Before and after COVID-19 Lockdown periods, where pollution levels exhibited notable variations due to human and economic activities (Laxmipriya & Narayanan 2021).

Performance of the three time series modelling methods is compared based on the AQI data of three monitoring stations in Chennai city, Velachery, Alandur and Manali. Section 2 presents an overview of the study area and statistical descriptions of the data. The methodology followed in the three methods and the performance measures considered for comparison are outlined in Section 3. Time series models are constructed based on the AQI values collected from each of the three monitoring stations, applying the three model-building methods in Section 4. Performance of the models is also compared for each monitoring station for before and after the COVID-19 lockdown. Section 5 presents the concluding remarks.

STUDY AREA AND DATA DESCRIPTION

Study Area

Chennai is one of the four major metropolitan cities in India and is the capital of Tamil Nadu state. The population size of this city is increasing mainly due to the growth of the manufacturing and Information Technology industries,

which is leading to an influx of people from other cities and neighboring states. As reported by the Tamil Nadu Pollution Control Board 2021 (Sekar et al. 2020), the population density of the city is 26,553 people per square kilometer. The Central Pollution Control Board (CPCB) of India operates three continuous ambient air quality monitoring stations in the city at Velachery, Alandur and Manali. Velachery is a commercial and residential area located in the southern part of Chennai, Alandur is a residential area in the southwest of the city, and Manali is an industrial area located in the northern part of Chennai. These stations record daily data on levels of pollutants for the respective region, such as PM2.5, NO, NO_2, NOx, NH_3, SO_3, O_3, Benzene and Toluene, as well as meteorological factors such as wind speed, direction, relative humidity and temperature. In each station, as per the guidelines of CPCB, the sub-indices are computed every day for each chemical pollutant, and the highest sub-index is determined as the value of AQI of the region.

Data Description

The AQI data was collected from Velachery monitoring station for a period of 813 days from January 1, 2018 to April 24, 2020; from Alandur monitoring station for a period of 1178 days from January 1, 2017 to March 24, 2020 and from Manali monitoring station for a period of 479 days from December 1, 2018 to April 24, 2020. All these time series contain missing values and outliers. The occurrence of missing observations in a dataset is not uncommon. It is due to the missing records caused by phenomena, faulty equipment, loss of records, or a mistake that cannot be rectified. When one or more observations are missing, it may be necessary to replace them with suitable estimates. Such replacements can provide a better understanding of the nature of the data. Some of the standard ways of handling missing data include deleting and imputation (The missing values are either left out or replaced with a single substitute). In time series, the temporal dependency is essential and deleting values may interrupt this continuity and replacement methods may change the original time series, causing reduced statistical power and biased estimations. Missing values in a time series can make it difficult to determine correlations with past lag, and the presence of outliers in the data may lead to biased forecasting results. This can be overcome by the replacement of appropriate values in the positions of missing observations and by suitable estimates in the positions of outliers.

Kihoro et al. (2013) suggested that model-based estimation methods can be more statistical, which can be followed to determine such values. Here, the LSTM model-based method is applied to determine such replacement values and estimates.

Plot of the AQI data for the three locations - Velachery, Alandur and Manali - is displayed in Fig. 1. The figure enables to identification of patterns and trends in the AQI data over time for each location. The figure reveals that the plot of AQI of Velachery has spikes in June, October and November of 2018, followed by a decreasing trend in 2019. The plot of AQI of Alandur exhibits an upward trend in AQI at the end of each year, with relatively little fluctuation during other periods. The plot of the AQI of Manali shows a moderate downward trend in AQI over the years.

Table 1 presents statistical information about the AQI of the three different locations. The levels of AQI in Velachery range from 17.50 to 194.09, with a mean value of 63.77 and a standard deviation of 29.69. Twenty-five percent of the values of AQI in Velachery lie below 41.00; half of the information lies below/above the median value of 57.05, and the remaining twenty-five percent of the values lie above 79.72. From the coefficient of skewness and coefficient of kurtosis, respectively 1.23 and 1.70, it can be noted that the distribution for AQI could be positively skewed and platykurtic.

The levels of AQI in Alandur range from 19.50 to 378.19, with a mean value of 83.70 and a standard deviation of 39.01. Twenty-five percent of the values of AQI in Alandur lie below 60.11; half of the information lies below/above the median value of 76.02, and the remaining twenty-five percent of the values lie above 95.07. The coefficient of skewness and coefficient of kurtosis, respectively 1.55 and 4.15, point out that the distribution for AQI could be positively skewed and leptokurtic.

The levels of AQI in Manali range from 16.54 to 351.61, with a mean value of 117.10 and a standard deviation of 66.04. Twenty-five percent of the values of AQI in Manali lie below 70.62; half of the information lies below/above the median value of 96.08, and the remaining twenty-five percent of the values lie above 145.00. The coefficient of skewness

Table 1: Descriptive Statistical Measures.

Statistical Measure	Velachery	Alandur	Manali
Minimum	17.50	19.50	16.54
Maximum	194.09	378.19	351.61
Mean	63.77	83.70	117.10
Median	57.05	76.02	96.08
Standard Deviation	29.69	39.01	66.04
Quartile 1	41.00	60.11	70.62
Quartile 3	79.72	95.07	145.00
Coefficient of Variation	0.47	0.47	0.56
Coefficient of Skewness	1.23	1.55	1.53
Coefficient of Kurtosis	1.70	4.15	2.01

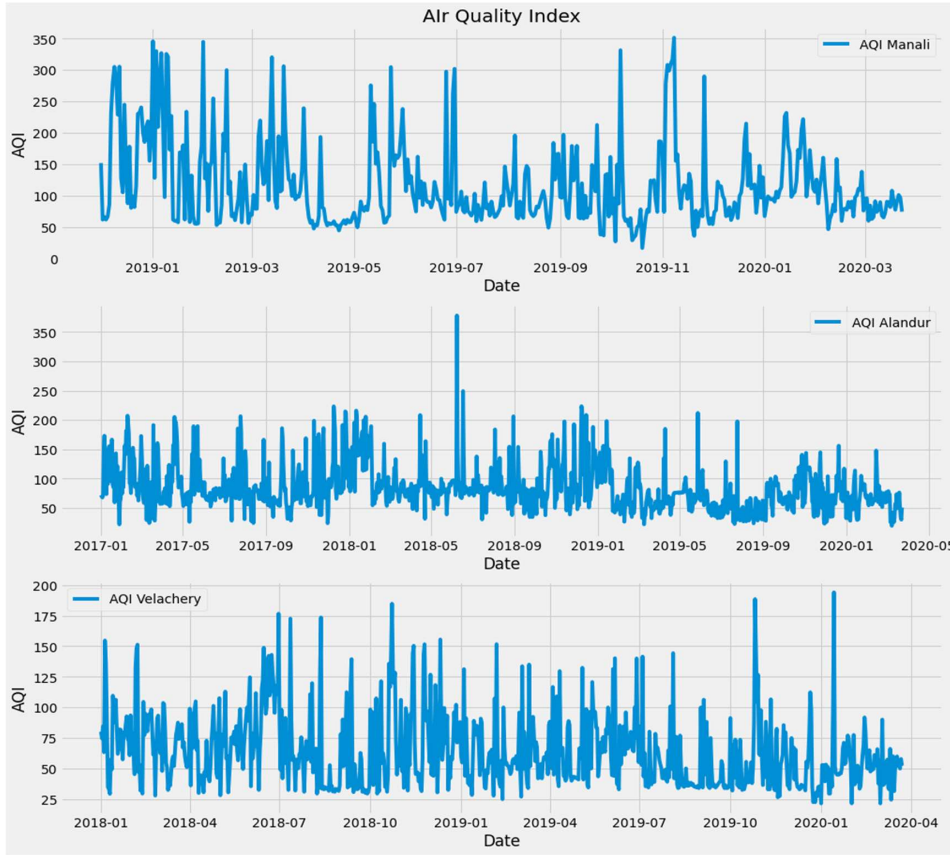

Fig. 1: AQI of Velachery, Alandur and Manali Stations.

and coefficient of kurtosis are 1.53 and 2.01respectively, which suggests that the distribution for AQI in Manali could be positively skewed and leptokurtic.

The coefficient of variation for AQI of Velachery, Alandur and Manali is 47%, 47% and 56% respectively. These indicate that consistency in the time series of AQI of Velachery and Alandur is equal and is relatively more consistent than the time series of AQI of Manali.

According to the categorization of National Air Quality Index consideration range (https://app.cpcbccr.com/ccr/#/login), the average air quality in Velachery and Alandur is Satisfactory, and in Manali is moderately polluted.

MATERIALS AND METHODS

Autoregressive Moving Average Method

The ARMA model is estimated for a given time series by applying the Box-Jenkins approach to predict the values for future periods (Box et al., 1970). The general form of the ARMA model is given by:

$$y_t = \alpha + \beta_1 y_{t-1} + \beta_2 y_{t-2} + \ldots + \beta_p y_{t-p} + e + \phi_1 \varepsilon_{t-1} + \phi_2 \varepsilon_{t-2} + \ldots + \phi_q \varepsilon_{t-q}$$

Where,

y_t is the observation of time t

α is the intercept

β_i is the coefficient of the autoregressive (AR) component with lag t-i, i=1, 2, 3, …, p

ϕ_j is the coefficient of the moving average (MA) component with lag t-j, j=1, 2, 3, …, q

Determination of the coefficients □, $\square_i$ (i=1, 2, 3, …, p) and $\square_j$ (j=1, 2, 3, …, q) The given time series is popularly known as fitting of the ARMA(p, q) model. Various unit root tests are applied to evaluate the stationarity of a given time series statistically, before determining the estimates. The Dickey-Fuller test is a commonly used test of this type, which tests:

H_{01}: The Time series is not stationary

against

H_{11}: The Time series is stationary.

If the value of the test statistic is significant, the series can be considered stationary. The Ljung–Box test is applied to determine if there is any significant autocorrelation in the given time series, which tests the hypotheses.

H_{02}: Residuals are independently distributed

against

H_{12}: Residuals are not independently distributed.

Optimal values of p and q for the ARMA model can be determined from the values of AIC and BIC. It is generally recommended to choose the combination of p and q corresponding to the relatively lower values of AIC or BIC. The plots of the values of the autocorrelation function (ACF) and the partial autocorrelation function (PACF) are also considered for diagnosing the values of p and q.

Facebook Prophet Method

The Facebook Prophet model decomposes a time series into three components, viz., trend, seasonality and holidays. The trend component captures the overall direction and level of the time series, while the seasonality component captures periodic fluctuations in the data. The holiday component is used to model the effect of special events or holidays in the time series data. Together, these three components can be used to model and forecast future values of the time series. The general form of the Facebook Prophet model is given by (Taylor & Letham 2018).

$$y(t) = g(t) + s(t) + h(t) + \epsilon_t$$

where

y(t) represents the time-dependent response variable,

g(t) is the trend function,

s(t) is the seasonality component,

h(t) represents the holiday effect, and ϵ_t is the measure of overall uncertainty in the model.

By choosing change points from the data, a piecewise linear trend automatically finds changes in trends, and its form is:

$$g(t) = \left[\left(k + \sum_{i \geq t} \delta_i\right) t + m + \sum_{i \geq t} (-\text{change point}_i \delta_i)\right] \times y_{scaled}$$

Where k is the growth rate, d is the rate adjustment, m is the offset parameter and y_{scaled} is the time series data that has been scaled (normalized) to have values between 0 and 1. This is done to make the data easier to work with and to ensure that the trends and seasonality are not affected by the scale of the data.

The seasonality component is modelled using the Fourier series as

$$s(t) = \sum_{j=1}^{n} \left(a_n \cos\left(\frac{2\pi jt}{P}\right) + b_n \sin\left(\frac{2\pi jt}{P}\right)\right)$$

Where P is the regular period determining the periodic fluctuations in the data. A high value of P indicates strong seasonality, while a low value indicates weak seasonality.

The holiday component h(t) refers to specific days of the year that deviate from the normal schedule or routine, such as holidays or special events. These days are predictable and they occur at the same time every year.

In the general form, ϵ_t represents the uncertainty or error in the model prediction for time t. It is used to model the variability or noise in the data, which the model is trying to predict. It is important to note that the value of ϵ_t will vary over time, depending on the data being used and the model performance. Taylor and Letham (2018) have mentioned that a low value of indicates a more accurate prediction, and a high value indicates greater uncertainty.

Long Short-Term Memory Method

The LSTM method was proposed by Hochreiter & Schmidhuber (1997), which is one of the methods developed applying the deep learning approach for fitting linear and nonlinear stationary time series models. The LSTM model can identify long-range patterns in the time series.

As described by Van Houdt et al. (2020), the LSTM method functions with three gates, viz., the input gate, forget gate and output gate. This method functions in the three gates with a set of equations as explained below:

The LSTM unit gets the current input sequence, given by x^t, and the output from the preceding time step, denoted by h^{t-1}. The weighted inputs are added together and then transferred through a tanh activation to produce $\widetilde{C_t}$ as:

$$\widetilde{C_t} = \tanh(W_c x^t + U_c h^{t-1} + b_c)$$

The input gate directs the flow of data into the memory cell through the sigmoid activation function.

$$i_t = \sigma(W_i x^t + U_i h^{t-1} + b_i)$$

The forget gate reads x^t and h^{t-1} and activates weighted inputs with the sigmoid function. The forget gate f_t is multiplied by the cell state at the preceding time step C^{t-1}, allowing the memory contents, which are no longer considered forgotten.

$$f_t = \sigma(W_f x^t + U_f h^{t-1} + b_f)$$

The output gate uses a sigmoid activation function to regulate the information flows out of the LSTM unit by taking the weighted sum of x^t and h^{t-1}.

$$O_t = \sigma(W_O x^t + U_O h^{t-1} + b_O)$$

The current cell state C_t is calculated by ignoring irrelevant information from the preceding time step and accepting relevant information from the current input. This is mainly composed of the constant error carousel, which has a recurring edge with unit weight.

$$C_t = \widetilde{C_t} \times i_t + C_{t-1} \times f_t$$

By transferring the cell state C_t through a tanh function and multiplying i_t with the output gate O_t, the LSTM unit output, h_t, is calculated from

$$h_t = \tanh(C_t) \times O_t$$

Where,

$x^t \in \mathbb{R}^d$ is the input vector for the LSTM unit,

$f_t \in \mathbb{R}^h$ is the forget gate activation vector,

$i_t \in \mathbb{R}^h$ is the input/update gate activation vector,

$O_t \in \mathbb{R}^h$ is the output gate activation vector,

$h^t \in \mathbb{R}^h$ is the hidden state vector,

$\widetilde{C_t} \in \mathbb{R}^h$ is the cell input activation vector,

$C_t \in \mathbb{R}^h$ is the cell state vector and

$W \in \mathbb{R}^{h*d}$, $U \in \mathbb{R}^{h*h}$ and $b \in \mathbb{R}^h$ are respectively the input weight, recurrent weight and bias vector.

Here, d and h refer to the number of input features and the number of hidden units, respectively, and is the sigmoid activation function.

The LSTM network architecture was carefully designed based on our data characteristics and experimental validation, with key architectural decisions focused on balancing complexity and efficiency. A three-layer structure was implemented, beginning with an input layer of 50 neurons to process initial data, followed by a hidden layer of 50 neurons to capture intermediate patterns, and concluding with an output layer containing neurons aligned with the prediction horizon. Hyperparameters were rigorously justified to optimize performance: the memory cells integrated three sigmoid layers and one tanh layer to regulate information flow, while a learning rate of 0.001 ensured stable convergence during training. A batch size of 32 samples was selected to balance computational efficiency and gradient stability, and a dropout rate of 0.2 was applied to minimize overfitting risks. These design choices collectively aimed to enhance the model's predictive accuracy while maintaining computational practicality.

Model Evaluation Measures

The train-test split of the time series is implemented to assess the model's effectiveness with unseen data. By training the model on a portion of the data and evaluating its performance on a separate portion with test data, a better understanding can be gained of how the model will perform for other datasets. If the model performs well on the test data, confidence can be placed in the ability of the model to perform well on future data (Briggs et al. 1999).

In the present study, the AQI recorded in the three monitoring stations is split into training (95%) and test (5%) data. In the Velachery monitoring station, the AQI from 01-01-2018 to 11-02-2020 is considered as the training data, and the AQI from 12-02-2020 to 23-03-2020 is considered as the test data. For the Alandur monitoring station, the AQI from 01-01-2017 to 24-02-2020 is considered as the training data, and the AQI from 25-01-2020 to 23-03-2020 is considered as the test data. For the Manali monitoring station, the AQI from 12-01-2018 to 28-02-2020 is considered as the training data, and the AQI from 29-02-2020 to 23-03-2020 is considered as the test data.

The 5% test split, though small in proportion, represents over one month of contiguous daily data, ensuring sufficient temporal coverage for statistically meaningful evaluation. Forecasting beyond one month in a daily time series introduces significant challenges due to error accumulation and increased uncertainty, as small deviations compound over time, reducing prediction reliability. The test period maintains a balance between robust validation and minimizing the risk of error propagation, ensuring the model's performance metrics remain interpretable and representative of real-world forecasting scenarios (Briggs et al. 1999).

Toharudin et al. (2020) have stated that mean absolute error (MAE), root mean squared error (RMSE), and mean absolute percentage error(MAPE) are commonly used measures to assess a model's predictive capability. These measures are used here to evaluate the model performance and to make model comparisons (Zhang et al. 2013). Values of these measures can be calculated for a given time series using the following formulae.

$$\text{MAE} = \frac{1}{n}\sum_{t=1}^{n}\left|Y_t - \widehat{Y_t}\right|$$

$$\text{MAPE} = \frac{1}{n}\sum_{t=1}^{n}\left|\frac{Y_t - \widehat{Y_t}}{Y_t}\right|$$

$$\text{RMSE} = \sqrt{\frac{1}{n}\sum_{t=1}^{n}\left(Y_t - \widehat{Y_t}\right)^2}$$

Y_t is the actual value at time t.

$\hat{Y}_t$ is the estimated value at time t.

n is the number of observations.

The MAE measures the average magnitude of the errors in a model's predictions, whereas RMSE considers the average squared difference between the predicted and actual values. MAPE provides a relative measure, which is useful for comparing across datasets with different scales.

TIME SERIES MODELS AND EVALUATION

Time Series Models for AQI of Velachery

ARMA model for Velachery: The stationarity of the time series of AQI recorded in the Velachery monitoring station is tested by applying the Dickey-Fuller test. The p-value of the test statistic is computed as 0.0019, which indicates that the time series of AQI recorded in the Velachery monitoring station can be stationary. The order of the ARMA model for this time series can be diagnosed from the ACF and PACF plots displayed in Fig. 2.

The ACF plot shows that the first 20 lags are significant, and the PACF plot indicates that lags 1, 5 and 13 are significant. The ARMA models are estimated corresponding to each pair (p, q) with p = (1, 2, 3, 13) and q = (1, 2, 3). The values of AIC and BIC are calculated for each ARMA model and are displayed in Table 2.

It can be noted from Table 2 that the smallest value of BIC, 159.11, is obtained corresponding to the ARMA (2,1) model, whereas the smallest value of AIC, 134.34, is obtained corresponding to the ARMA (3,2) model. The p-values calculated for the construction of the ARMA (2,1) model reveal that the model is not significant for the time series considered. The results corresponding to the construction of the ARMA (3,2) model are presented in Table 3.

Table 2: AIC and BIC Values for ARMA Models of Velachery Station.

S. No.	p	q	AIC	BIC
1.	1	1	147.468	166.064
2.	1	2	148.380	171.625
3.	1	3	146.436	174.330
4.	2	1	135.86	159.11
5.	2	2	136.74	164.64
6.	2	3	137.47	170.02
7.	3	1	136.59	164.48
8.	3	2	134.34	166.88
9.	3	3	136.17	173.36
10.	13	1	145.31	219.69
11.	13	2	146.428	225.461
12.	13	3	147.803	231.485

Table 3: ARMA (3,2) Model for AQI of Velachery.

p-value of Dickey-Fuller Test	Fitted Model	α	β_1, β_2 and β_3 Co-efficients	ϕ_1, ϕ_2 and ϕ_3 Co-efficients
0.0019	ARMA (3,2)	4.07	2.54, -2.19 and 0.65	-1.78 and 0.83

The estimated ARMA model for the time series of AQI recorded in the Velachery monitoring station is

$$y_t = 4.07 + 2.54 * y_{t-1} - 2.19 * y_{t-2} + 0.65 * y_{t-3} - 1.78\varepsilon_{t-1} + 0.83\varepsilon_{t-2}$$

Value of the Ljung–Box test statistic for lag of 20 is calculated as 14.47 with p-value of 0.80. It indicates that there is no significant evidence to determine that the residuals are autocorrelated at a lag of 20.

Prophet model for Velachery: The Prophet model is fitted by considering a linear trend growth and taking into account forty-eight days from Jun 2022 to December 2022 declared as public holidays by the Tamil Nadu Government. The maximum change point is set at 0.09. The overall trend in the values of AQI of Velachery station during the study period is displayed in Fig. 3. The plot also shows the yearly trend, holiday, weekly, and yearly seasonality in the values of AQI. The pattern of the trend in the values of the AQI shows a decreasing tendency over the period mentioned above. The weekly trend is almost zero on all days, except Tuesday. The weekly trend increases from Sundays and reaches a peak on Tuesdays, which gradually falls from Wednesdays. Thursdays and Fridays show a shallow increase from Wednesdays and rise higher on Saturdays. Analysis of the yearly trend shows the highest levels of AQI at the end of June and the lowest levels during October. Spikes can be noted on holidays, which point out the influence on the values during the respective holidays.

The estimated trend function of the Prophet model for the AQI of Velachery station is:

$$g(t)=\left[\left(-0.14+\sum_{i\geq t}\delta_i\right)+0.40+\sum_{i\geq t}(-\text{change point}_i\times\delta_i)\right]\times y_{scaled}$$

LSTM model for Velachery: Determination of the LSTM model for the time series of AQI of Velachery station shall be treated as a supervised learning problem, applying the Min-Max scaling to reduce the influence of outliers. As there is no definite method for determining the appropriate number of neurons in a neural network, in this study, the model, with five hidden layers containing 50 neurons each, is employed. The batch size, or the number of inputs processed at one time,

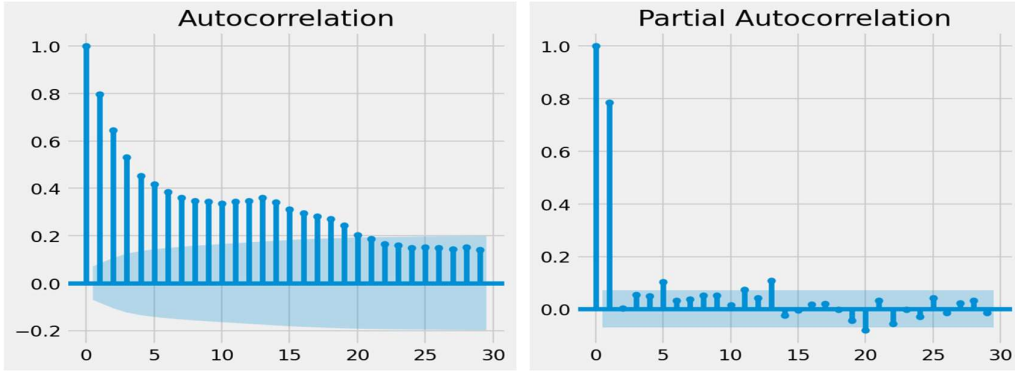

Fig. 2: ACF and PACF plots of AQI of Velachery station.

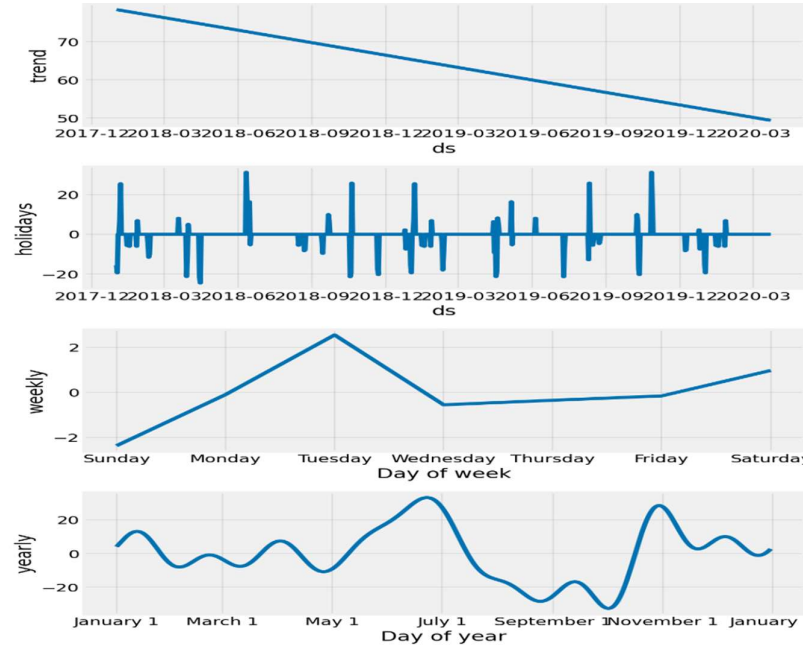

Fig. 3: Yearly, Weekly trends and Holiday effects fitted for Velachery.

is set to 100, and the model is run for 100 epochs. Thus, orders of the parameters of the input gate, forget gate, cell state, and output gate of the LSTM network are:

$W_{i,f,c,o}$ is a vector of order 1×50,

$U_{i,f,c,o}$ is a matrix of order 50×50,

$b_{i,f,c,o}$ It is a vector of order 1×50.

Here, the subscripts i, f, c and o represent, respectively input gate, forget gate, cell state and output gate. Also, the weights and biases are used to control the flow of information into the LSTM unit and are updated during the training process.

Evaluation of Time Series Models for AQI of Velachery Station

Values of the performance evaluation measures, MAE, MAPE and RMSE, are computed for the estimated ARMA, Prophet and LSTM models based on the test data of AQI of Velachery station. The values are presented in Table 4 under the column head "Before COVID-19 Lockdown". Values of the evaluation measures show that among the three models, the LSTM model has the lowest error rate with an MAE of 10.26 and an RMSE of 13.05. The difference between the error rates of Prophet and ARMA models is very marginal.

The MAE and RMSE of the Prophet model are respectively 13.30 and 17.11, whereas the MAE and RMSE of the estimated ARMA model are respectively 13.88 and 18.81. These values indicate that among the three models, the accuracy level in the forecast values obtained from the estimated LSTM is relatively higher. Also, there could be a

margin of difference in the accuracy level of the predicted values given by the ARMA and Prophet models.

MAPE indicates that the LSTM model achieves the highest accuracy, with the lowest error of 0.24. In comparison, the ARMA model exhibits an MAPE of 0.41, representing a 70.83% increase relative to the LSTM model, while the Prophet model shows an MAPE of 0.31. The ARMA model's error is 32.26% higher than that of the Prophet model and 70.83% higher than that of the LSTM model. These findings demonstrate that the LSTM model outperforms both the ARMA and Prophet models, establishing it as the most reliable approach, whereas the ARMA model exhibits the highest error among the three.

The observed and the estimated values of the test data of AQI of Velachery station for the "Before COVID-19 Lockdown" period, i.e., from 12-02-2020 to 23-03-2020, are plotted in Fig. 4. The observed values are depicted by a solid blue line; the estimated AQI values from the ARMA model by a dashed red line; the estimated AQI values from the Prophet model by a dash-dot-dash green line; and the estimated AQI values from the LSTM model by a dotted magenta line. It can be noticed from Fig. 4, the estimated values from the ARMA and Prophet models deviate much from the respective observed values. The estimated values from the LSTM model are relatively close to the observed values.

Similar analysis is carried out for the "After COVID-19 Lockdown" period training data from June 1, 2022, to November 07, 2022, and test data from November 08, 2022, to December 05, 2022. Values of MAE and RMSE

Table 4: MAE and RMSE Values of Time Series Models for Velachery Station.

Performance Measure	Before COVID19 Lockdown			Post COVID19 Lockdown		
	ARMA	Prophet	LSTM	ARMA	Prophet	LSTM
MAE	13.88	13.30	10.26	19.01	18.67	13.52
RMSE	18.81	17.11	13.05	24.46	23.97	16.92
MAPE	0.41	0.31	0.24	0.25	0.25	0.21

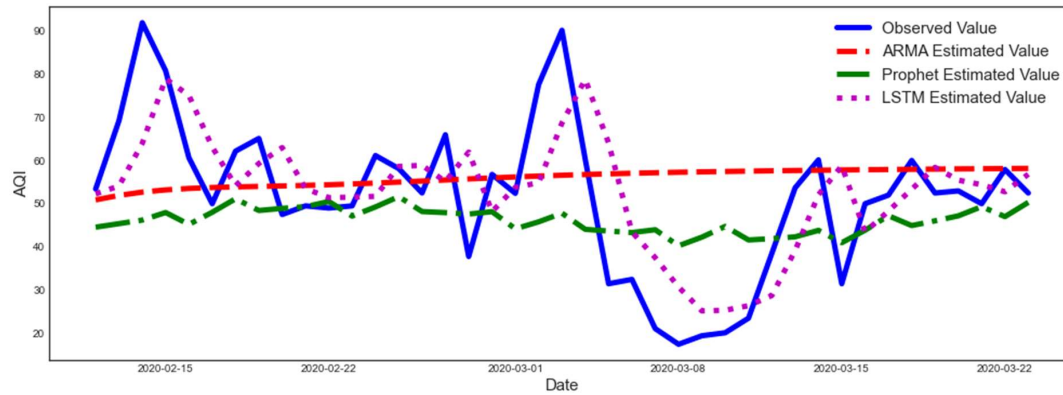

Fig. 4: Observed and Estimated Values of AQI from ARMA, Prophet and LSTM Models for Velachery Station (Before COVID-19 Lockdown).

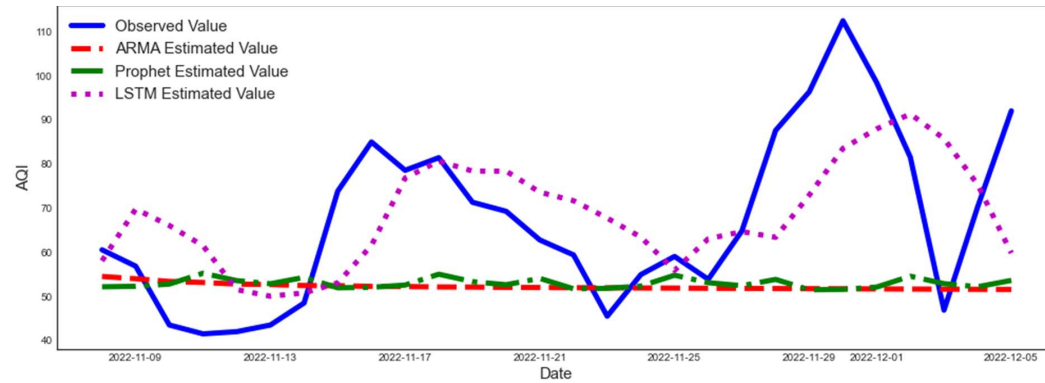

Fig. 5: Observed and Estimated Values of AQI from ARMA, Prophet and LSTM Models for Velachery Station (Post COVID-19 Lockdown).

calculated from the estimated ARMA, Prophet and LSTM models are presented in Table 4 under the column head "Post COVID-19 Lockdown". The tendency in the error rates of the three models is similar to that of the "Before COVID-19 Lockdown" period. The MAE and RMSE for the LSTM model are 13.52 and 16.92, respectively, which are smaller than the corresponding MAE and RMSE for the ARMA and Prophet models. The observed and the estimated values plotted in Fig. 5 also exhibit this fact.

The LSTM model continues to demonstrate the highest accuracy, with the lowest MAPE of 0.21. In comparison, both the ARMA and Prophet models exhibit an MAPE of 0.25, which represents a 19.05% increase in error relative to the LSTM model. It can be inferred from all these facts that the LSTM method of constructing a time series model can provide a relatively more appropriate time series model for the AQI of the Velachery monitoring station.

Time Series Modelling for AQI of Alandur

ARMA model for Alandur: The stationarity of the time series of AQI recorded in the Alandur monitoring station is tested by applying the Dickey-Fuller test. The p-value of the test statistic is computed as 0.0, which indicates that the time series of AQI recorded in the Alandur monitoring station can be stationary.

The order of the ARMA model for this time series can be diagnosed from the ACF and PACF plots displayed in Fig. 6. The ACF plot indicates that all lags are significant, and the PACF plot indicates that lags 1, 2, 3, and 5 are significant. The ARMA models are estimated corresponding to each pair (p, q) with p = (1, 2, 3, 5) and q = (1, 2, 3). The values of AIC and BIC are calculated for each ARMA model and are displayed in Table 6. It can be noted from Table 5 that the smallest values of AIC 905.663 and BIC 935.784 are obtained, corresponding to the ARMA model (3, 1) is presented in Table 6. The estimated ARMA model for the time series of AQI recorded in the Alandur monitoring station is:

Table 5: AIC and BIC Values for ARMA Models of Alandur Station.

S. No.	p	q	AIC	BIC
1.	1	1	921.91	941.998
2.	1	2	916.187	941.28
3.	1	3	912.845	942.966
4.	2	1	909.872	934.973
5.	2	2	911.572	936.975
6.	2	3	909.872	934.973
7.	3	1	905.663	935.784
8.	3	2	906.764	937.642
9.	3	3	906.985	936.224

Table 6: ARMA (3, 1) Model for AQI of Alandur.

ADF test p-value	Fitted Model	Constant	b – Coefficient	Coefficient
0.0	ARMA (3,1)	4.34	1.32, -0.24 and -0.09	-0.92

$$y_t = 4.34 + 1.32 \times y_{t-1} - 0.24 \times y_{t-2} - 0.09 y_{t-3} - 0.92 \varepsilon_{t-1}$$

Value of the Ljung–Box test statistic for lag of 20 is calculated as 14.48 with p-value of 0.81. It indicates that there is no significant evidence to determine that the residuals are autocorrelated at a lag of 20.

FB Prophet Model for Alandur: The Prophet model is fitted by considering a linear trend and taking into account seventy-four days from January 2017 to March 2020 declared as public holidays by the Tamil Nadu Government. The maximum change point was set at 0.09. The overall trend in the values of AQI of Alandur station during the study period is displayed in Fig. 7.

The plot also shows the yearly trend, holiday, weekly, and yearly seasonality in the values of AQI. The pattern of trend in the values of AQI shows a decreasing tendency over the period mentioned above. The spikes can point out the

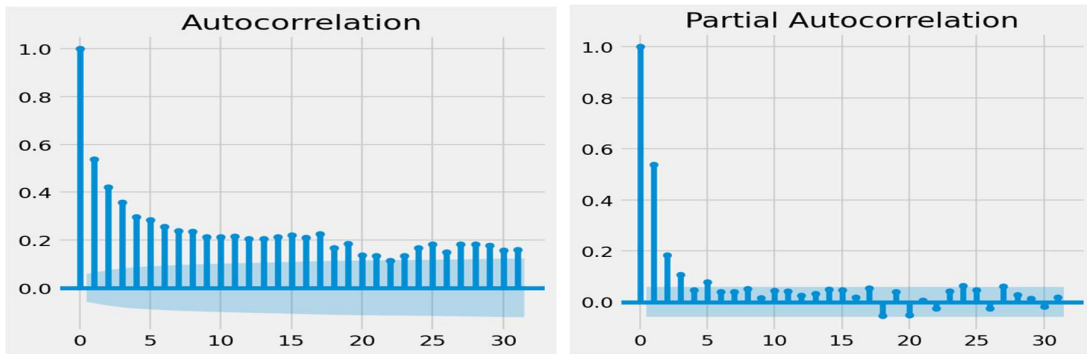

Fig. 6: ACF and PACF plot of AQI of Alandur station.

influence on the values during the respective holidays. The weekly trend increases from Thursdays and reaches a peak on Friday, which gradually falls from Saturdays. Analysis of the yearly seasonality indicates the highest level of AQI during the beginning of January and the end of October, and the lowest levels during March.

The estimated trend component of the Prophet model for the AQI of the Alandur station is:

$$\text{Trend } g(t) = \left[\left(-0.095 + \sum_{i \geq t} \delta_i\right) + 0.206 + \sum_{i \geq t}(-\text{change point}_i \times \delta_i)\right] \times y_{scaled}$$

LSTM model for Alandur: Determination of the LSTM model for the time series of AQI of Alandur station shall be treated as a supervised learning problem, applying the Min-Max scaling to reduce the influence of outliers. The model with five hidden layers containing 70 neurons each is employed. The batch size, or the number of inputs processed at one time, is set to 100, and the model is run for 100 epochs. Thus, orders of the parameters of the input gate, forget gate, cell state, and output gate of the LSTM network are:

$W_{i,f,c,o}$ is a vector of order 1×70

$U_{i,f,c,o}$ is a matrix of order 70×70

$b_{i,f,c,o}$ It is a vector of order 1×70

Here, the subscripts i, f, c and o represent, respectively input gate, forget gate, cell state and output gate. Also, the weights and biases are used to control the flow of information into the LSTM unit and are updated during the training process.

Model Evaluation for the Alandur Time Series

Values of the performance evaluation measures, MAE and RMSE, are computed for the estimated ARMA, Prophet and LSTM models based on the test data of AQI of Alandur station and are presented in Table 7. The values are presented in Table 7 under the column head "Before COVID-19 Lockdown". Values of the evaluation measures show that among the three models, the LSTM model has the lowest error rate with an

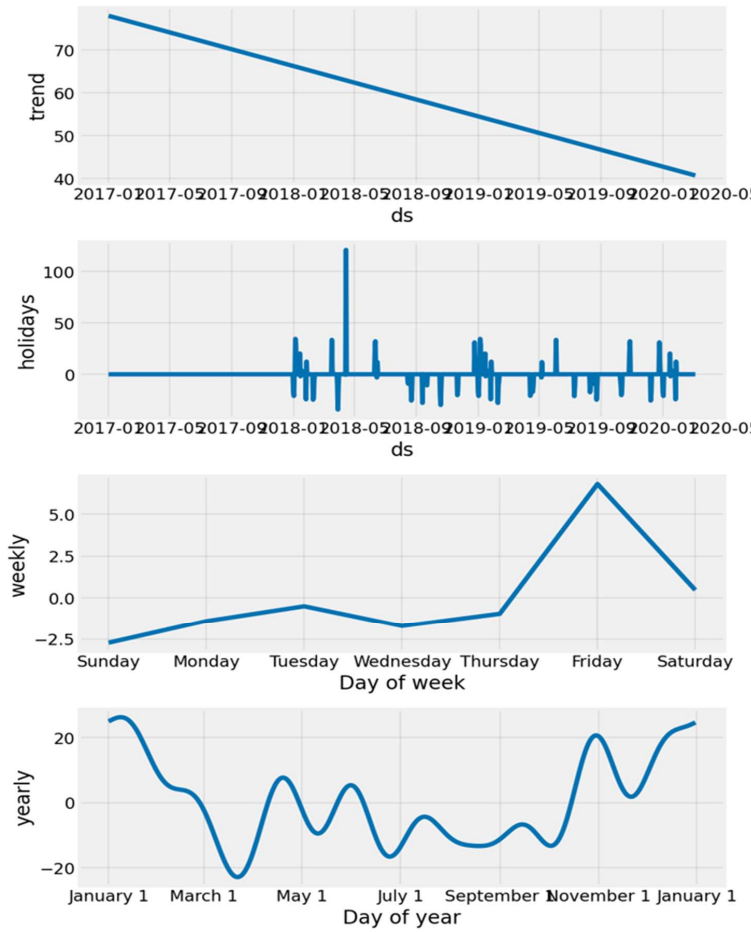

Fig. 7: yearly, monthly, weekly trends and holiday plot for Alandur.

MAE of 12.58 and an RMSE of 17.58. The ARMA model has the highest error rate with an MAE of 16.23 and an RMSE of 22.90. The MAE and RMSE of the estimated Prophet model are smaller than the respective values of the estimated ARMA model. The MAE and RMSE of the Prophet model are, respectively, 13.60 and 18.17, which are lower than the ARMA model, but higher than the LSTM model. The difference between the error rates of LSTM and ARMA models is relatively high. The LSTM and Prophet models demonstrated comparable accuracy, both achieving the lowest MAPE values of 0.25. In contrast, the ARMA model exhibited the highest error, with an MAPE of 0.36, which is 44% higher than that of the LSTM and Prophet models.

These values indicate that among the three models, the accuracy level in the forecast values obtained from the estimated LSTM is relatively higher. Also, there could be a margin of difference in the accuracy level of the predicted values given by the LSTM and Prophet models.

The observed and the estimated values of the test data of AQI of Alandur station for the "Before COVID-19 Lockdown" period, i.e., from 24-01-2020 to 23-03-2020, are plotted in Fig. 8. The observed values are depicted by a solid blue line; the estimated AQI values from the ARMA model by a dashed red line; the estimated AQI values from the Prophet model by a dash-dot-dash green line; and the estimated AQI values from the LSTM model by a dotted

Table 7: MAE and RMSE for Alandur Time Series.

Station/Model	Error Measures	Before COVID COVID-19 lockdown			Post-COVID-19 Lockdown		
		ARMA	Prophet	LSTM	ARMA	Prophet	LSTM
Alandur	MAE	16.23	13.60	12.58	30.72	33.79	27.66
	RMSE	22.90	18.17	17.58	37.84	38.59	37.14
	MAPE	0.36	0.25	0.25	0.32	0.37	0.26

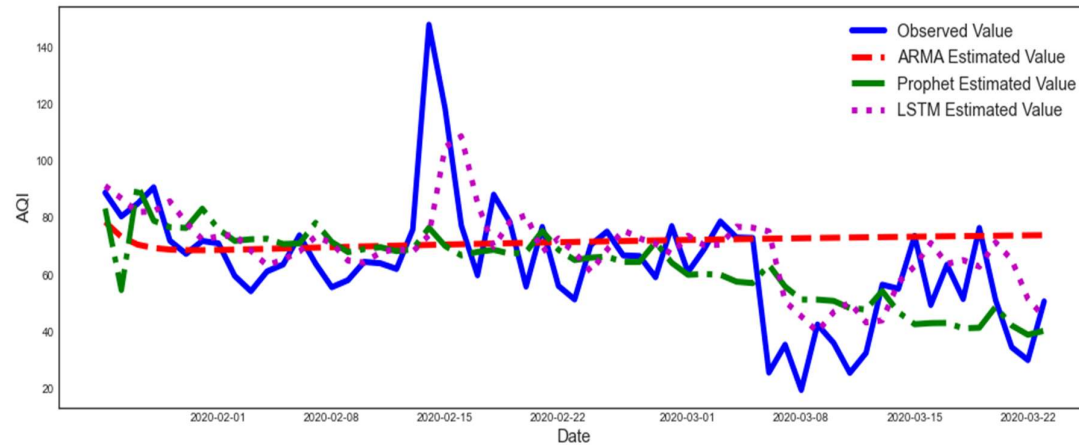

Fig. 8: Observed and estimated values of AQI from ARMA, Prophet and LSTM Models for Alandur station (Before COVID-19 Lockdown).

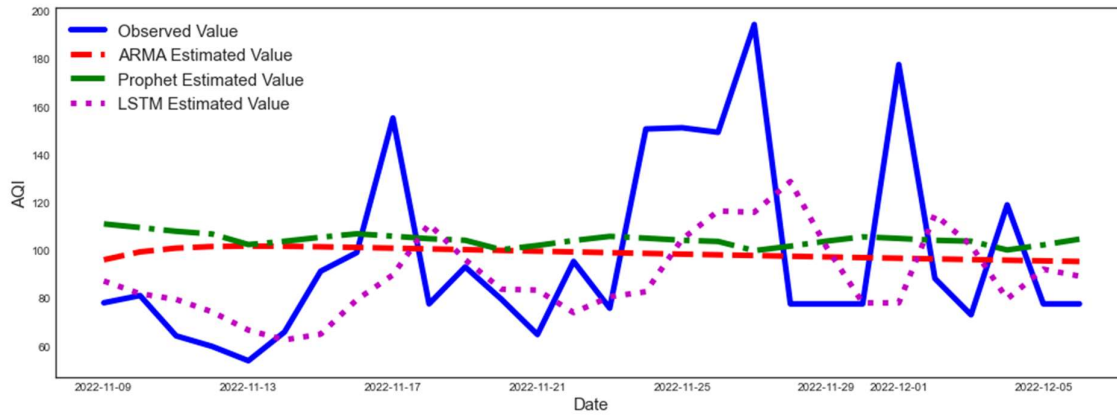

Fig. 9: Observed and estimated values of AQI from ARMA, Prophet, and LSTM Models for Alandur station (Post-COVID-19 Lockdown).

magenta line. It can be noticed from Fig. 8, the estimated values from the ARMA and Prophet models deviate much from the respective observed values. The estimated values from the LSTM model are relatively close to the observed values.

Similar analysis is carried out for the "After COVID-19 Lockdown" period with training data from June 1, 2022, to November 07, 2022, and test data from November 08, 2022, to December 05, 2022.

Values of MAE and RMSE calculated from the estimated ARMA, Prophet, and LSTM models are presented in Table 7 under the column head "Post COVID-19 Lockdown". The tendency in the error rates of the three models is similar to that of the "Before COVID-19 Lockdown" period.

The MAE and RMSE for the LSTM model are 27.66 and 37.14, respectively, which are smaller than the corresponding MAE and RMSE for the ARMA and Prophet models. The observed, and the estimated values plotted in Fig. 9 also exhibit this fact.

The MAE and RMSE for the LSTM model are 27.66 and 37.14, respectively, which are smaller than the MAE and RMSE for the ARMA and Prophet models. The LSTM model maintained its consistent performance, achieving the lowest MAPE of 0.26. However, the Prophet model's error increased significantly to 0.37, making it the least accurate among the three models. The ARMA model showed a slight improvement, with its MAPE decreasing to 0.32, but it still exhibited a 23.08% higher error compared to the LSTM model.

It can be inferred from all these facts that the LSTM method of constructing a time series model can provide a relatively more appropriate time series model for the AQI of the Alandur monitoring station.

Table 8: AIC and BIC Values for the ARMA Model of Manali Station.

S. No	p	q	AIC	BIC
1.	1	1	544.892	557.253
2.	1	2	528.378	544.860
3.	2	1	507.393	507.393
4.	2	2	503.755	524.356

Time Series Modelling for AQI of Manali

ARMA model for Manali: The stationarity of the time series of AQI recorded in the Velachery monitoring station is tested by applying the Dickey-Fuller test. The p-value of the test statistic is computed as 0.0003, which indicates that the time series of AQI recorded in the Manali monitoring station can be stationary. The order of the ARMA model for this time series can be diagnosed from the ACF and PACF plots displayed in Fig. 10.

The ACF plot indicated that lags 1 and 2 are significant, and the PACF plot showed that lags 1 and 2 are significant. The ARMA models are estimated corresponding to each pair (p, q) with p = (1, 2) and q = (1, 2). The values of AIC and BIC are calculated for each ARMA model and are displayed in Table 8.

It can be noted from Table 8 that the smallest value of AIC and BIC is obtained corresponding to the ARMA (1, 2) are presented in Table 9, which are respectively 528.38 and 544.86.

The estimated ARMA model for the time series of AQI recorded in the Manali monitoring station is:

$$y_t = 0.18 + 0.99 \times y_{t-1} - 0.49\varepsilon_{t-1} - 0.21\ \varepsilon_{t-2}$$

Value of the Ljung–Box test statistic for lag of 20 is calculated as 23.842 with p value of 0.24. It indicates that

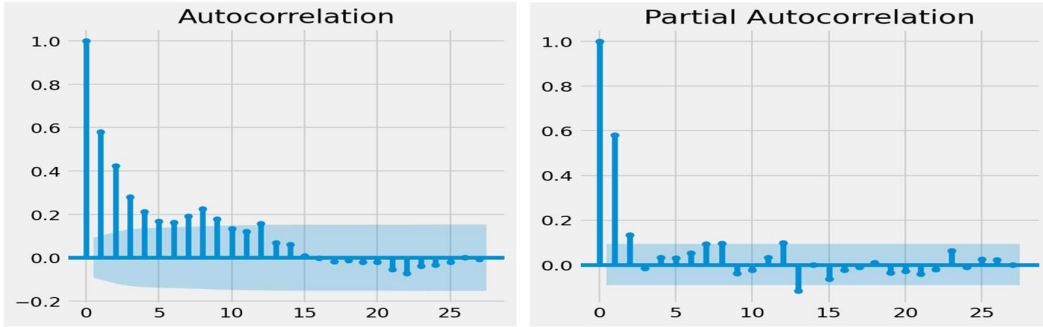

Fig. 10: ACF and PACF plot for Manali.

Table 9: ARMA (1, 2) Model for AQI of Manali.

Time Series	ADF test p-value	Fitted Model	Constant	β – Coefficient	Φ –Coefficient
Manali	0.0003	ARMA (1,2)	0.18	0.99	-0.49 and -0.22

there is no significant evidence to determine that the residuals are autocorrelated at a lag of 20.

FB Prophet for Manali: The Prophet model is fitted by considering a linear trend growth and taking into account twenty-eight days from December 2018 to April 2020, declared as public holidays by the Tamil Nadu Government. The maximum change point is set at 0.09. The overall trend in the values of AQI of Manali station during the study period is displayed in Fig. 11. The plot also shows the yearly trend, weekly, holiday, and yearly seasonality in the values of AQI.

The yearly trend indicates, pattern of trend in values of the AQI shows a decreasing tendency over the period of mentioned above. The weekly trend showed that AQI values increase from Sunday and reach a peak on Thursday. The yearly seasonality revealed that the highest levels of AQI occur during the first half of October and November, and the lowest levels of AQI occur during the end of March and April. Spikes can be noted on holidays, which indicate the influence on the values during the respective holidays.

The estimated trend function of the Prophet model for the AQI of the Manali station is

$$\text{Trend } g(t) = \left[\left(-0.14186748 + \sum_{i \geq t} \delta_i\right) + 0.40382178 + \sum_{i \geq t} (-\text{change point}_i \times \delta_i)\right] \times y_{\text{scaled}}$$

LSTM Model for Manali: This study, a model that employs multiple hidden layers, with five hidden layers containing 50 neurons each. The batch size, or the number of inputs processed at one time, is set to 50, and the model is run for 63 epochs. Thus, orders of the parameters of the input gate, forget gate, cell state and output gate of the LSTM network are:

$W_{i,f,c,o}$ is a vector of order 1×50

$U_{i,f,c,o}$ is a matrix of order 50×50

$b_{i,f,c,o}$ is a vector of order 1×50

Here, the subscripts i, f, c and o represent, respectively input gate, forget gate, cell state and output gate. Also, the weights and biases are used to control the flow of information into the LSTM unit and are updated during the training process. The input gate, forget gate, cell state and output gate weights are listed below.

Evaluation of Time Series Model for AQI of Manali Station: Values of the performance evaluation measures, MAE and RMSE, are computed for the estimated ARMA, Prophet and LSTM models based on the test data of AQI

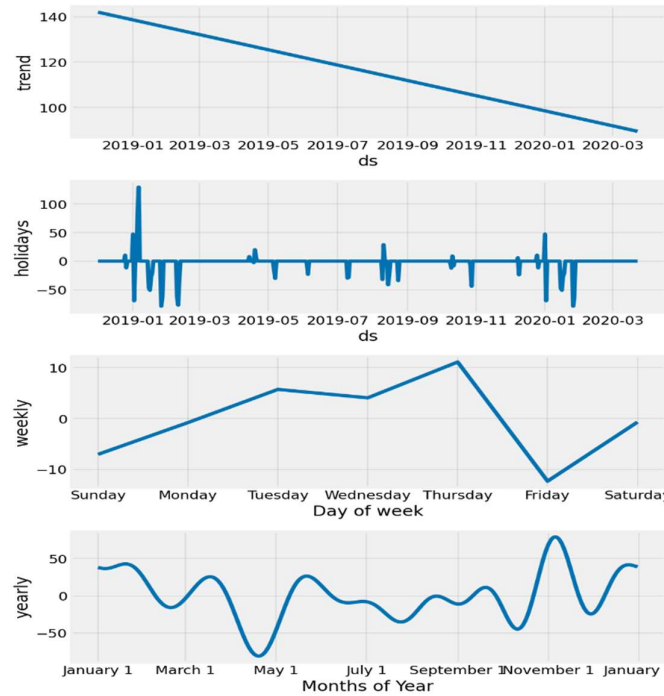

Fig. 11: Yearly, weekly trends and holiday effects fitted for Manali.

Table 10: MAE and RMSE Values of Time Series for Manali Station.

Station/Model	Error Measures	Before COVID COVID-19 lockdown			Post-COVID-19 Lockdown		
		ARMA	Prophet	LSTM	ARMA	Prophet	LSTM
Manali	MAE	21.79	24.83	11.75	17.33	15.09	14.95
	RMSE	25.25	28.62	13.68	24.25	21.53	21.65
	MAPE	0.30	0.33	0.15	0.18	0.15	0.16

of the Manali station. The values are presented in Table 10 under the column head "Before COVID-19 Lockdown".

Values of the evaluation measures show that among the three models, the LSTM model has the lowest error rate with an MAE of 11.75 and an RMSE of 13.68. The difference between the error rates of Prophet and ARMA models is marginal. The MAE and RMSE of the Prophet model are respectively 24.83 and 28.62, whereas the MAE and RMSE of the estimated ARMA model are respectively 21.79 and 25.25. These values indicate that among the three models, the accuracy level in the forecast values obtained from the estimated LSTM is relatively higher. Also, there could be a margin of difference in the accuracy level of the predicted values given by the ARMA and Prophet models.

The LSTM model has the lowest error rate with an MAPE of 0.15. In contrast, the Prophet model had the highest error, with an MAPE of 0.33, followed by the ARMA model with an MAPE of 0.30. These findings indicate that the LSTM model was the most reliable before the COVID-19 lockdown period.

The observed and the estimated values of the test data of AQI of Manali station for the "Before COVID-19 Lockdown" period, i.e., from 29-02-2020 to 23-03-2020, are plotted in Fig. 12. The observed values are depicted by a solid blue line; the estimated AQI values from the ARMA model by a dashed red line; the estimated AQI values from the Prophet model by–a dash-dot-dash green line; and the estimated AQI values from the LSTM model by a dotted magenta line. It can be noticed from Fig. 12, the estimated values from the ARMA and Prophet models are far from the respective observed values. The estimated values from the LSTM model are relatively close to the observed values.

Similar analysis is carried out for the "After COVID-19 Lockdown" period with training data from June 1, 2022, to November 07, 2022, and test data from November 08, 2022, to December 05, 2022. Values of MAE and RMSE calculated from the estimated ARMA, Prophet, and LSTM models are presented in Table 10 under the column head "Post COVID-19 Lockdown". The tendency in the error rates of the three models is similar to that of the "Before COVID-19 Lockdown" period.

The MAE and RMSE for the LSTM model are 17.33 and 24.25, respectively, which are smaller than the corresponding MAE and RMSE for the ARMA and Prophet models. The observed, and the estimated values plotted in Fig. 13 also exhibit this fact. The difference between the error rates of LSTM and the Prophet model is marginal. In the post-lockdown period, all models demonstrated improved accuracy. The Prophet model achieved the lowest MAPE of 0.15, followed closely by the LSTM model with 0.16, while the ARMA model recorded a MAPE of 0.18. Compared to the pre-lockdown period, the ARMA and Prophet models

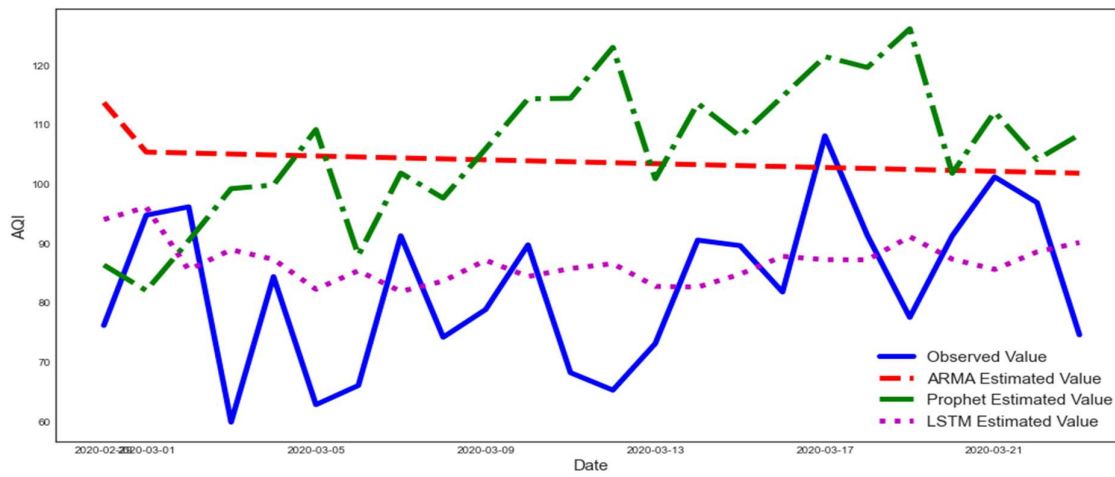

Fig. 12: Observed and Estimated Values of AQI from ARMA, Prophet and LSTM Models for Velachery Station (Before COVID-19 Lockdown).

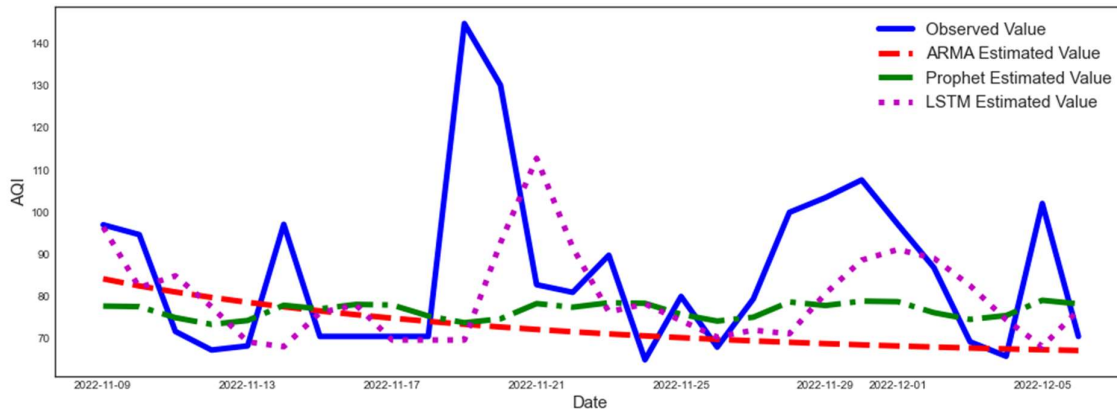

Fig. 13: Observed and Estimated Values of AQI from ARMA, Prophet, and LSTM Models for Velachery station (Post COVID-19 Lockdown).

showed notable improvements, while the LSTM model's error slightly increased.

It can be inferred from all these facts that the LSTM method of constructing a time series model can provide a relatively more appropriate time series model for the AQI of the Manali monitoring station.

CONCLUSIONS

Time series models have a special feature of forecasting the observations for future periods. They play a vital role in many fields, particularly in forecasting the economy, demography, and environment of a country. Several methods have been developed with different approaches, and the performance of the methods is found to vary with respect to the data.

An empirical study is carried out in this work to compare the performance of the ARMA method developed in the statistical approach, the Prophet method developed employing a Machine Learning procedure, and the long short-term memory method developed employing Deep Learning methodology. Time series models are constructed for daily air quality indices observed before and after COVID COVID-19 lockdown periods of three locations of Chennai city. Among the three methods, the long short-term memory method performs relatively better than the other two methods for the three time series with respect to measures of accuracy in forecast values. The performance of the ARMA method and the Prophet method depends on the data set. Results do not differ, except for numerical values, for pre- and post-COVID-19 lockdown periods.

REFERENCES

Abhilash, M.S.K., Thakur, A., Gupta, D. and Sreevidya, B., 2018. *Ambient Communications and Computer Systems*. Springer, pp. 413–426.

Ammasi Krishnan, M., Devaraj, T., Velayutham, K., Perumal, V. and Subramanian, S., 2020. Statistical evaluation of PM2.5 and dissemination of PM2.5, SO2 and NO2 during Diwali at Chennai, India. *Natural Hazards*, 103(3), pp.3847–3861.

Anand Kumar Varma, S., Mahmood Anas, M.S., Harun Raseed, M., Nithishbalasubramanian, O. and Madhan Kumar, R., 2021. Determination of air quality index and its impacts on human health in Chennai City. *Magna Scientia Advanced Research and Reviews*, 3(1), p.76. DOI

Angelena, J.P., Stanley Raj, A., Viswanath, J. and Muthuraj, D., 2021. Evaluation and forecasting of PM10 air pollution in Chennai district using wavelets, ARIMA, and neural network algorithms. *Pollution*, 7(1), pp.55–72.

Box, G.E.P., Jenkins, G.M. and Reinsel, G., 1970. *Time Series Analysis: Forecasting and Control*. Holden-Day, San Francisco.

Briggs, W.M., Makridakis, S., Wheelwright, S.C., Hyndman, R.J. and Diebold, F.X., 1999. Forecasting: Methods and applications. *Journal of the American Statistical Association*, 26, p.917. DOI

Büyükşahin, Ü.Ç. and Ertekin, Ş., 2019. Improving forecasting accuracy of time series data using a new ARIMA-ANN hybrid method and empirical mode decomposition. *Neurocomputing*, 361, pp.151–163. DOI

Calvo, B. and Santafé Rodrigo, G., 2016. Scmamp: Statistical comparison of multiple algorithms in multiple problems. *The R Journal*, 8(1), pp.248–256.

Gunasekar, S., Joselin Retna Kumar, G. and Dileep Kumar, Y., 2022. Sustainable optimized LSTM-based intelligent system for air quality prediction in Chennai. *Acta Geophysica*, 71, p.96. DOI

Haviluddin, Alfred, R., Obit, J.H., Hijazi, M.H.A. and Ibrahim, A.A.A., 2015. A performance comparison of statistical and machine learning techniques in learning time series data. *Advanced Science Letters*, 21(10), pp.3073–3076. DOI

Hochreiter, S. and Schmidhuber, J., 1997. Long short-term memory. *Neural computation*, 9(8), pp.1735-1780.

Janarthanan, R., Partheeban, P., Somasundaram, K. and Navin Elamparithi, P., 2021. A deep learning approach for the prediction of air quality index in a metropolitan city. *Sustainable Cities and Society*, 67, p.102720. DOI

Kihoro, J.M., Athiany, H., Walter, O.Y. and W, K.H., 2013. Imputation of incomplete non-stationary seasonal time series data. *Journal of Time Series Analysis*, 3(12), pp.201–210.

Laxmipriya, S. and Narayanan, R.M., 2021. COVID-19 and its relationship to particulate matter pollution – case study from part of Greater Chennai, India. *Materials Today: Proceedings*, 43, pp.1634–1639.

Loganathan, A., Sumithra, P. and Deneshkumar, V., 2022. Estimation of air quality index using multiple linear regression. *AEES*, *10*, pp.717-722.

Mani, G. and Volety, R., 2021. A comparative analysis of LSTM and ARIMA for enhanced real-time air pollutant levels forecasting using

sensor fusion with ground station data. *Cogent Engineering*, 8(1), pp.90. DOI

Nadeem, I., Ilyas, A.M. and Sheik Uduman, P.S., 2020. Analyzing and forecasting the ambient air quality of Chennai City in India. *Geography, Environment, Sustainability*, 13(3), pp.13–21. DOI

Naveen, V. and Anu, N., 2017. Time series analysis to forecast air quality indices in Thiruvananthapuram District, Kerala, India. *Journal of Engineering Research and Applications*, 7(6), pp.66–84.

Parmezan, A.R.S., Souza, V.M.A. and Batista, G.E.A.P.A., 2019. Evaluation of statistical and machine learning models for time series prediction: Identifying the state-of-the-art and the best conditions for the use of each model. *Information Sciences*, 484, pp.302–337. DOI

Patra, S.R., 2017. Time series forecasting of air pollutant concentration levels using machine learning. *Advances in Computer Science and Information Technology*, 4(5), pp.280–284.

Samal, K.K.R., Babu, K.S., Das, S.K. and Acharya, A., 2019. Time series-based air pollution forecasting using SARIMA and the Prophet model. *ACM International Conference Proceeding Series,* 91, pp.646-672. DOI

Samia, A., Kaouther, N. and Abdelwahed, T., 2012. A hybrid ARIMA and artificial neural networks model to forecast air quality in urban areas: case of Tunisia. *Advanced Materials Research*. 34, pp.2969–2979.

Sánchez-Pozo, N.N., Trilles-Oliver, S., Solé-Ribalta, A., Lorente-Leyva, L.L., Mayorca-Torres, D. and Peluffo-Ordóñez, D.H., 2021. *Algorithms for Air Quality Estimation: A Comparative Study of Stochastic And Heuristic Predictive Models*. In the Springer, pp.293–304.

Sekar, T., Venkatachalam, A.V.V. and Kallolikar, S., 2020. Impact of COVID-19 lockdown on the air quality of Chennai. *Environmental Studies Journal*, 12(2), pp.101–110.

Taylor, S.J. and Letham, B., 2018. Forecasting at scale. *American Statistician*, 72(1), pp.37–45. DOI

Toharudin, T., Pontoh, R.S., Caraka, R.E., Zahroh, S., Lee, Y. and Chen, R.C., 2020. Employing long short-term memory and the Facebook Prophet model in air temperature forecasting. *Communications in Statistics: Simulation and Computation*. 44, pp.21-36. DOI

Van Houdt, G., Mosquera, C. and Nápoles, G., 2020. A review on the long short-term memory model. *Artificial intelligence review*, *53*(8), pp.5929-5955.

Zhang, X., Liu, Y., Yang, M., Zhang, T., Young, A.A. and Li, X., 2013. Comparative study of four time series methods in forecasting typhoid fever incidence in China. *PLoS One*, 8(5), p.e63116.